Published in final edited form as:
J Vasc Interv Radiol. 2010 August ; 21(8): 1255–1261. doi:10.1016/j.jvir.2010.02.043.

Increased expression of HIF-1α, VEGF-A and its receptors, MMP-2, TIMP-1, and ADAMTS-1 at the venous stenosis of arteriovenous fistula in a mouse model with renal insufficiency

Sanjay Misra, MD, **Uday Shergill, MBBS**, **Binxia Yang, MD, PhD**, **Rajiv Janardhanan, PhD**, and **Khamal D. Misra, BSN**
Department of Radiology, Mayo Clinic College of Medicine, Rochester, Minnesota

Abstract

Purpose—A mouse model of renal insufficiency with arteriovenous fistula (AVF) and venous stenosis was created. We tested the hypothesis that there is increased gene expression of hypoxia inducible factor-1 alpha (HIF-1α), vascular endothelial growth factor- A (VEGF-A) and its receptors (VEGFR-1, -2), matrix metalloproteinase-2 (MMP-2), -9 (MMP-9), tissue inhibitor of metalloproteinase-1, -2 (TIMP-1, -2), and a disintegrin and metalloproteinase thrombospondin-1 (ADAMTS-1) at the venous stenosis.

Materials and methods—Nineteen male C57BL/6 mice underwent a left nephrectomy and a surgical occlusion of the right upper pole to induce renal insufficiency and characterized in eight mice. Twenty eight days later, an AVF (n=11) was created from the right carotid artery to ipsilateral jugular vein and the mice were sacrificed at day 7 (n=4) and day 14 (n=4). The outflow and control veins were removed for gene expression. Three mice were sacrificed at day 28 for histologic analysis.

Results—The mean serum blood urea nitrogen remained significantly elevated for 8 weeks when compared to baseline ($P<0.05$). By day 7, there was a significant increase in the expression of HIF-1α, VEGF-A, VEGFR-1, VEGFR-2, MMP-2, TIMP-1, and ADAMTS-1 at the outflow vein with HIF-1α and TIMP-1 being significantly elevated at day 14 ($P<0.05$). By day 28, the venous stenosis was characterized by a thickened vein wall and neointima.

Conclusions—A mouse model of renal insufficiency with AVF was developed which had increased expression of HIF-1α, VEGF-A, VEGFR-1, VEGFR-2, MMP-2, TIMP-1, and ADAMTS-1 at the outflow vein with venous stenosis by day 28.

Introduction

Maintaining vascular access patency is essential to patients with endstage renal disease (ESRD) because it allows for the optimal delivery of hemodialysis. The arteriovenous fistula (AVF) is the preferred vascular access, however, its patency at one year is estimated to be

Corresponding author: Sanjay Misra, M.D., Associate Professor, Department of Radiology, Mayo Clinic College of Medicine, 200 First Street SW, Alfred 6460, Rochester, MN 55905, Telephone: 507-255-7208, Fax: 507-255-7872, misra.sanjay@mayo.edu.

The authors have no conflicts of interest.

This work was presented at the 35Th Annual meeting of the Society of Interventional Radiology in Tampa, Florida.

only 62% [1]. Data suggests that AVF fail because of venous stenosis formation caused by intimal hyperplasia [2]. Histologic analysis of specimens removed from patients with failed vascular accesses reveal that there is evidence of angiogenesis with intimal hyperplasia located within the neointima and adventitia. These observations from clinical specimens suggest that angiogenesis with matrix deposition and cellular proliferation play an important role in the pathophysiology of hemodialysis vascular access graft failure [3]. Therefore, understanding the mechanisms which lead to the formation of venous stenosis is of critical importance in developing strategies that delay or prevent graft failure.

Hypoxia is a fundamental stimulus for modulating the expression of angiogenic and matrix regulatory proteins which are responsible for mediating angiogenesis, matrix deposition, cellular proliferation, and migration. Increased hypoxia mediates expression of hypoxia inducible factor-1 alpha (HIF-1α), a transcription factor which results in increased expression of vascular endothelial growth factor-A (VEGF-A), matrix metalloproteinases (MMPs), and ADAMTS-1 [4]. A recent study showed that HIF-1α was significantly increased in specimens removed from patients with failed hemodialysis vascular access and in our porcine model of hemodialysis graft failure [5]. Taken collectively, these observations suggest that hypoxia plays a critical role in neointimal formation in hemodialysis graft failure.

Intimal hyperplasia is produced by the proliferation of vascular smooth muscle cells together with matrix deposition [3]. While various cytokines have been implicated in this process, one that may be of particular importance is vascular endothelial growth factor-A. This is because VEGF-A is important in vascular remodeling and restenosis, and because its expression is increased in patients with failed grafts [6]. However, because these observations are from clinical specimens that are at the end stage of the venous stenotic and thrombotic process, it is not clear whether the increased VEGF contributed to the development of the intimal hyperplasia or was a result of the advanced process. Previous studies have demonstrated that there is increased VEGF-A expression at the venous stenosis in a porcine model of hemodialysis graft failure [7].

Another group of cytokines that are thought to play a key role in hemodialysis graft failure are the matrix metalloproteinases (MMPs) and their endogenous inhibitors, tissue inhibitors of matrix metalloproteinase (TIMPs) [8]. This is based on the observation that an imbalance of MMP activity over TIMPs promotes migration and proliferation of smooth muscle cells, and that certain MMPs increase the bioavailability of VEGF-A, potentially accelerating the development of intimal hyperplasia [9]. Previous studies support a prominent role for MMPs in hemodialysis graft failure; we reported that PTFE grafts in pigs exhibited early up-regulation of MMP-2 associated with increased cell migration from the adventitia to the media and intima, and subsequent formation of venous stenosis [10]. Furthermore, non-specific MMP-2 and MMP-9 inhibitors reduced the formation of neointima in the same model [11]. Thus, these studies suggest that MMPs (specifically MMP-2 and MMP-9) may play a prominent role in the pathogenesis of intimal hyperplasia of hemodialysis grafts. Recently a new family of metalloproteinases has been discovered, a disintegrin and metalloproteinase thrombospondins (ADAMTs) which has been shown to be increased in specimens removed from patients with hemodialysis grafts [12]. Finally, there is interaction between ADAMTS-1, MMP-9, and VEGF-A [9,13].

Animal models have been developed in order to understand the mechanisms responsible for hemodialysis vascular access failure. To date, much of the experimental research performed in hemodialysis vascular access has been performed in animal models with normal kidney function which does not adequately simulate the clinical scenario [11,14,15]. It is well recognized that patients with chronic renal insufficiency have increased oxidative stress; and

that oxidative stress is associated with increased expression of VEGF-A, MMPs, and other proteins [16]. Recently, several groups have described a murine model of AVF which venous stenosis formed at the outflow vein [17,18]. The aim of the present study was to develop a murine model of renal insufficiency with an AVF and venous stenosis to better simulate the clinical scenario. The second aim was to determine the expression of HIF-1α and genes which are regulated by HIF-1α and know to have increased expression in hemodialysis vascular access including VEGF-A and its receptors, MMP-2, MMP-9, TIMP-1, TIMP-2, and ADAMTS-1 [5–7,10–12]. Finally, the histologic changes at the venous stenosis and control vein at day 28 after fistula creation were characterized.

Materials and methods

Study design

Our Institutional Animal Care and Use Committee approval was obtained prior to performing any procedures on animals. The housing and handling of the animals was performed in accordance with the Public Health Service Policy on Humane Care and Use of Laboratory Animals revised in 2000 [19]. Nineteen male C57BL/6 mice (Jackson Laboratories, Bar Harbor, ME) weighing 25–30 grams were used. Nephrectomy was created by removing the left kidney and ligating the blood supply to the upper pole of the right kidney. In eight mice, the kidney function was determined by measuring serum blood urea nitrogen and creatinine at baseline and 1, 2, 5, 6, and 8 weeks after nephrectomy. Four weeks after nephrectomy, AVFs were created in eleven mice from the right carotid artery to the ipsilateral jugular vein and the contralateral vessels served as controls. Eight mice were sacrificed at day 7 (N=4) and day 14 (N=4) following fistula creation for real time polymerase chain reaction (RT-PCR) analysis. An additional, three mice were sacrificed at day 28 following fistula creation for histologic analysis. The specimens were snap frozen in liquid nitrogen and stored at −80 °C in RNAse free conditions for RT-PCR analysis or were stored in formalin and embedded in paraffin for histologic analysis.

Nephrectomy in the mouse

Before experimentation, all animals were housed in a room with a 22°C temperature, 41% relative humidity, and 12-/12-hour light/dark cycles in the animal care wing and were allowed access to water and food ad libitum. Anesthesia was achieved with intraperitoneal injection of a mixture of ketamine hydrochloride (0.20 mg/g) and xylazine (0.02 mg/g) and maintained with intraperitoneal pentobarbital (20–40 mg/kg). After shaving and sterilely preparing the abdomen, the mice were fixed in a supine position. The operation was performed under a dissecting microscope (Zeiss Operating Microscope OPMI 6-SDFC, Oberkochen, Germany). An incision was made in the mid line of the abdomen and the left kidney was exposed. The artery, vein, and ureter to the left kidney were ligated, and the kidney was removed. Next, the renal arteries to the upper pole of the right kidney were surgically ligated so that approximately half of the right kidney remained. The mice after the surgery were maintained on regular diet for four weeks at which time a arteriovenous fistula was placed. Serum BUN and creatinine were measured by removing blood from the tail vein at baseline (before nephrectomy), 1, 2, 5, 6, and 8 weeks after nephrectomy. Four weeks after nephrectomy, an AVF was placed. The weight of the kidney at sacrifice and the weight of the mice weekly were determined.

Creation of arteriovenous fistula (AVF) in the mouse [18]

Four weeks after nephrectomy, the mice were fixed in a supine position and the neck was extended, shaved, and sterilely prepared. The operation was performed under a dissecting microscope. Through a midline skin incision of the neck, common carotid artery and ipsilateral external jugular vein were dissected and exposed. The cleidomastoid muscle was

resected. All branches of the jugular vein were ligated (ethilon 10-0, Ethicon, Somerville, NJ). The common carotid artery was clamped proximally, ligated just below the carotid bifurcation using an 8-0 ethilon and transected. The distal end was pulled through, inverted over and tied to the cuff which has an internal diameter of 0.28 mm and an outer diameter of 0.61-mm (Harvard Apparatus BS4 59-8321, Holliston, MA). The jugular vein was ligated distally and transected. The transected end was then placed over the cuff and tied with 8-0 ethilon circumference suture to form an end-to-end common carotid artery to jugular vein cuff anastomosis. The operative field and the vessel lumen were irrigated with a saline solution containing 100 IU/ml of heparin. The skin was then closed with continuous stitches using 6-0 vicryl. Mice were kept warm until complete recovery under a heating lamp, and 1.5 ml of saline solution was injected subcutaneously at the end of the procedure.

Tissue harvesting

At euthanasia, all mice were anesthetized as described previously and the fistula was dissected free of the surrounding tissue. Animals were euthanized by CO_2 asphyxiation and the outflow and control veins harvested for RT-PCR at day 7 and day 14 or histologic analyses at 28 days after the creation of the AVF. For RT-PCR analysis, control and outflow veins were harvested, immediately frozen in liquid nitrogen, and stored at −80°C for RT-PCR analysis in RNAse free tubes. For histological analysis, mice were perfused briefly (1 min) at 80 mm Hg with 0.9% NaCl solution via an abdominal aortic cannulation, and subsequently perfusion fixed with 4% phosphate-buffered formaldehyde (pH 7.2) for 15 min. Samples were fixed with 4% phosphate-buffered formaldehyde at 4°C for at least 24 h.

RNA isolation [18]

The tissue was stored in RNA stabilizing reagent (Qiagen, Gaithersburg, MD) as per the manufactures guidelines. To isolate the RNA, the specimens were homogenized and total RNA from the samples was isolated using RNeasy mini kit (Qiagen).

Real time polymerase chain reaction (RT-PCR) Analysis [18]

Briefly, first-strand complementary DNA (cDNA) was synthesized using Superscript III first strand (Invitrogen, Carlsbad, CA) according to the manufacturer's guidelines. cDNAs specific for the genes analyzed were amplified using the primers (see Table 1). PCR products were analyzed on 1.5% (w/v) agarose gels containing 0.5 μg/ml ethidium bromide. Bands were semiquantitated by scanning densitometry (Photoshop 5.5, Adobe, San Jose, CA). An area of the gel image that was devoid of signal was assigned to be the background value. Then each band representing the gene of interest was analyzed for the density above background at days 7 and 14 and then normalized to ensure that there were no differences in the amount of loading of mRNA to 18S gene and then pooled for all the animals.

Statistical methods

Comparisons between gene expression in the grafted vein and control vein of the mouse was performed using the Student's t-test and the Mann-Whitney test for parametric and nonparametric data respectively. Results are considered significant for P value less than or equal to 0.05. SAS version 9 (SAS Institute Inc., Cary, N.C.) was used for statistical analyses. Data are expressed as mean ± SD.

Results

Surgical outcomes

Nineteen mice underwent left nephrectomy and right upper pole occlusion followed by the creation of the arteriovenous fistula 28 days later from the right carotid artery to the

ipsilateral jugular vein twenty eight days later. Four mice were sacrificed at seven days and fourteen days later. Three animals were sacrificed at twenty eight days after the placement of the fistula for histologic analysis.

Serum BUN and creatinine changes after nephrectomy

The mean BUN and creatinine at baseline was 28 ± 5 mg/dL and 0.26 ± 0.1 mg/dL, respectively. The mean serum BUN was increased significantly at 1 (42 ± 7.8 mg/dL), 2 (52 ± 4.8 mg/dL), 5 (53 ± 11 mg/dL), 6 (43 ± 5.6 mg/dL), and 8 (56 ± 4.9 mg/dL) weeks after nephrectomy when compared to baseline ($P<0.05$). The mean serum creatinine was significantly increased at one (0.5 ± 0.01 mg/dL) and two (0.6 ± 0.1 mg/dL) weeks after nephrectomy when compared to baseline ($P<0.05$).

Weight of the kidney and mouse after nephrectomy

The mean weight of the remnant kidney at baseline was 222 ± 7 mg and it decreased to 192 ± 27 mg at 5-weeks and 175 ± 39 mg at 6-weeks ($P<0.05$ when compared to baseline). By 8-weeks, it was 190 ± 27 mg. The mean weight of the mouse at baseline was 23.3 ± 1.97 mg and remained relatively stable during the follow-up period. By eight weeks, the mean mouse weight was 28 ± 1.65 mg ($P<0.05$ when compared to baseline).

Gene expression of HIF-1α at the venous stenosis and control vein at day 7 and day 14

Gene expression for HIF-1α was determined by RT-PCR analysis on both the venous stenosis and control vessels. By day 7, the mean HIF-1α at the venous stenosis (1.71 ± 0.10) was significantly higher than the control vein (1.16 ± 0.36) and by day 14 remained slightly higher at the venous stenosis (1.10 ± 0.06, $P<0.05$) when compared to the control vein (0.92 ± 0.07, $P<0.05$) (Fig. 1).

Gene expression for VEGF-A and its receptors at the venous stenosis and control vein at day 7 and day 14

By day 7, the mean VEGF-Aat the outflow vein (1.78 ± 0.28) was significantly higher than the control vein (1.17 ± 0.45, $P<0.05$) and by day 14 decreased and was not different than the control vein (Fig. 2A). The mean VEGFR-1 expression at the venous stenosis (0.73 ± 0.13) was significantly higher than the control vein (0.39 ± 0.18, $P<0.05$) by day 7 which decreased by day 14 and was not different than the control vein (Fig. 2B). The mean VEGFR-2 expression at the venous stenosis (1.25 ± 0.25) was significantly higher than the control vein (0.98 ± 0.19, $P<0.05$) by day 7 which decreased by day 14 and was not different than the control vein (Fig. 2C). Overall, these results show that by day 7, there is increased expression of VEGF-A and its receptors at the venous stenosis when compared to the control vein.

Gene expression of MMP-2, MMP-9, TIMP-1, and TIMP-2 at the venous stenosis and control vein at day 7 and day 14

Gene expression for MMP-2, MMP-9, TIMP-1, and TIMP-2 was determined by RT-PCR analysis on both the venous stenosis and control vessels. By day 7, the mean MMP-2 expresssion at the venous stenosis (2.39 ± 0.23) was significantly higher than the control vein (1.2 ± 0.24, $P<0.05$) and by day 14 had become the same as the control vein (Fig. 3A). The mean TIMP-1 expression (1.98 ± 0.29) at the venous stenosis was higher than the control vein by day 7 (0.44 ± 0.26, $P<0.05$) which remained slightly higher in the venous stenosis when compared to the control vein by day 14 (1.02 ± 0.11, 0.8 ± 0.14, respectively, $P<0.05$) (Fig. 3B). There was no difference in the expression of MMP-9 and TIMP-2 between the venous stenosis and control vein at day 7 or day 14.

Gene expression of ADAMTS-1 at the venous stenosis and control vein at day 7 and day 14

Gene expression of ADAMTS-1 was determined by RT-PCR analysis on both the venous stenosis and control vessels. By day 7, the mean ADAMTS-1at the venous stenosis (1.23 ± 0.52) was significantly higher than the control vein (0.53 ± 0.05, $P<0.05$) and by day 14 there was no difference in the expression (Fig. 4).

Histologic analysis of venous stenosis and control veins at day 28

The histological changes were determined at the venous stenosis were characterized at day 28 after the fistula was created (Fig. 5). The wall of the venous wall was thicker than the control vein similar to the clinical scenario.

Discussion

The mechanisms underlying the formation of venous stenosis in hemodialysis graft failure remain poorly understood. Many factors have been hypothesized to be involved in the formation of venous stenosis including the expression of angiogenic and matrix regulatory proteins which may be a result of the increased HIF-1α at the venous anastomosis [5,20]. Animal models including the pig, rat, and mouse have been developed to test the role of these proteins in the formation of venous stenosis [10,18,21]. One major deficiency of these models has been that the animals have all had normal kidney function. It has been well documented that the uremic vascular environment is associated with increased oxidative stress and increased oxidative stress may be an important factor in the formation of intimal hyperplasia and venous stenosis [22,23]. Furthermore, many proteins which have been implicated in venous stenosis formation are also increased in conditions with increased oxidative stress including VEGF-A, bFGF, and PDGF [16]. Of note, all these proteins are also up regulated under hypoxic stimulus [4].

There are many models of renal insufficiency, which have been described including the mouse, rat, and pig [5,24–26]. In the present paper, we created a murine model of renal insufficiency prior to the placement of the arteriovenous fistula. After nephrectomy, we observed a period of acute renal failure which lasted two weeks and the kidney function began to improve. By four weeks, the mean serum BUN and creatinine had plateaued and remained stable until 8-weeks. These findings are consistent with our porcine model and the mouse remnant model described by Kren et al [24,25]. We also, observed a decrease in the remnant kidney weighs after nephrectomy with a slight decrease in the mouse weights after nephrectomy. Based on this data, we elected to place arteriovenous fistulas in the mouse four weeks after nephrectomy.

Hueper hypothesized that arterial hypoxia was involved in atherosclerosis [27]. Since then, the role of hypoxia has been expanded in vascular injury caused by atherosclerosis and restenosis [28]. Hypoxia is known to increase HIF-1α which is a potent regulator of many genes including VEGF-A, MMPs, and other genes [4]. Each of these proteins has been implicated in venous stenosis formation [10]. In the present study, we used RT-PCR analysis to determine HIF-1α expression and found it to be significantly up-regulated by day 7 and day 14 at the venous stenosis when compared to the control vein. This is consistent with previous studies that have demonstrated increased expression of HIF-1α in both failed hemodialysis vascular access grafts removed from patients and in a porcine model of hemodialysis graft failure [5,20].

Previous studies have focused on venous stenosis formation in hemodialysis graft failure by investigating the role of VEGF-A and matrix metalloproteinase [6]. In the present study, we observed significantly increased gene expression in VEGF-A, VEGFR-1, and VEGFR-2 at

the venous stenosis when compared to the control vein ($P<0.05$). This is consistent with observations made in a porcine model of hemodialysis graft failure where increased expression of VEGF-A, VEGFR-1, and VEGFR-2 was observed [7,20,21]. Furthermore, work by Roy Chaudhury and colleagues has demonstrated increased expression of VEGF-A in stenotic samples removed from patients with failed hemodialysis vascular access [6]. By day 14, the expression of these genes had decreased. This observation has therapeutic implications when considering the duration of anti-VEGF-A therapy which needs to be delivered.

Matrix metalloproteinase, specifically, MMP-2 and MMP-9 have been shown to be associated with venous stenosis formation in stenotic samples from patients with failed vascular access and animals models of hemodialysis vascular access failure [7,20,21]. In addition, VEGF-A and HIF-1α are known to regulate expression of MMPs. For this reason, we determined gene expression of MMP-2, MMP-9, and its inhibitors (TIMP-1 and TIMP-2) at the venous stenosis when compared to the control vein. We observed significantly increased gene expression of MMP-2 and TIMP-1 at the venous stenosis when compared to the control vein seven days after the placement of the arteriovenous fistula. By day 14, the expression of TIMP-1 remained significantly higher in the venous stenosis when compared to the control vein. These results are consistent with previous work from our laboratory in animal models of dialysis graft and fistula failure ans well as in specimens removed form patients with failed access [7,20]. In addition, these observations have therapeutic implications as they indicate that anti-MMP-2 therapy will be needed for approximately one week after fistula creation.

A recent study demonstrated that a new matrix metalloproteinase, ADAMTS-1 is increased significantly in specimens removed from patient with failed hemodialysis access grafts [12]. The role of ADAMTS-1 has been studied in a mouse carotid artery ligation model of arterial intimal hyperplasia [29]. In this model, transgenic mice which over expressed ADAMTS-1 were found to have increased amount of intimal hyperplasia of the carotid artery by day 14 when compared to controls. It has been hypothesized that ADAMTS-1 may modulate vascular smooth muscle cell migration in atherosclerosis and this may also be the case in hemodialysis vascular access. It has been shown that there is an increase in mRNA of ADAMTS-1 from human umbilical vein endothelial cells (HUVEC) and cardiac microvascular endothelial cells which have been exposed to shear stress [30]. Increased shear stress has been hypothesized as a potential etiology for hemodialysis graft failure [7,31,32]. In the present study, we observed significant increase in gene expression of ADAMTS-1 at the venous stenosis when compared to control vein by day 7.

In conclusion, we created a clinically relevant model of arteriovenous fistula failure in a mouse which the animals had abnormal kidney function. Using this model, we observed significant elevation of several important genes which have been implicated in venous stenosis formation including HIF-1α, VEGF-A, VEGFR-1, VEGFR-2, MMP-2, TIMP-1, and ADAMTS-1 with venous stenosis formation occurring by histologic analysis by day 28. Each of these genes has been associated with venosus stenosis formation. Future research will concentrate understanding the role of these genes by silencing their expression with lentivirus therapies or knockout models.

Acknowledgments

Funding: The project described was supported by Award Number R01HL098967 (SM) from the National Heart, Lung, And Blood Institute and a CR20 grant which is funded by 1UL1RR024150 from the National Center for Research Resources (NCRR), a component of the National Institutes of Health (NIH), and the NIH Roadmap for Medical Research. The content is solely the responsibility of the authors and does not necessarily represent the official views of the National Heart, Lung, And Blood Institute or the National Institutes of Health.

References

1. Rooijens PPGM, Tordoir JHM, Stijnen T, Burgmans JPJ, Smet de AAEA, Yo TI. Radiocephalic wrist arteriovenous fistula for hemodialysis: meta-analysis indicates a high primary failure rate. Eur J Vasc Endovasc Surg 2004;28:583–589. [PubMed: 15531191]
2. Sullivan KL, Besarab A, Bonn J, Shapiro MJ, Gardiner GA Jr, Moritz MJ. Hemodynamics of failing dialysis grafts. Radiology 1993;186:867–872. [PubMed: 8430200]
3. Rekhter M, Nicholls S, Ferguson M, Gordon D. Cell proliferation in human arteriovenous fistulas used for hemodialysis. Arterioscler Thromb 1993;13:609–617. [PubMed: 8096766]
4. Semenza GL. Targeting HIF-1 for cancer therapy. Nat Rev Cancer 2003;3:721–732. [PubMed: 13130303]
5. Misra S, Fu A, Pugionni A, et al. Increased expression of hypoxia inducible factor-1α in a porcine model of chronic renal insufficiency with arteriovenous polytetrafluoroethylene grafts. J Vasc Interv Radiol 2008;19:260–265. [PubMed: 18341959]
6. Roy-Chaudhury P, Kelly BS, Miller MA, et al. Venous neointimal hyperplasia in polytetrafluoroethylene dialysis grafts. Kidney Int 2001;59:2325–2334. [PubMed: 11380837]
7. Misra S, Fu AA, Puggioni A, et al. Increased shear stress with up regulation of VEGF-A and its receptors and MMP-2, MMP-9, and TIMP-1 in venous stenosis of hemodialysis grafts. Am J Physiol Heart Circ Physiol 2008;294:H2219–H2230. [PubMed: 18326810]
8. Loftus IM, Porter K, Peterson M, et al. MMP inhibition reduces intimal hyperplasia in a human vein graft stenosis model. Ann N Y Acad Sci 1999;878:547–550. [PubMed: 10415769]
9. Lee S, Jilani SM, Nikolova GV, Carpizo D, Iruela-Arispe ML. Processing of VEGF-A by matrix metalloproteinases regulates bioavailability and vascular patterning in tumors. J Cell Biol 2005;169:681–691. [PubMed: 15911882]
10. Misra S, Doherty MG, Woodrum D, et al. Adventitial remodeling with increased matrix metalloproteinase-2 activity in a porcine arteriovenous polytetrafluoroethylene grafts. Kidney Int 2005;68:2890–2900. [PubMed: 16316367]
11. Rotmans JI, Velema E, Verhagen HJ, et al. Matrix metalloproteinase inhibition reduces intimal hyperplasia in a porcine arteriovenous-graft model. J Vasc Surg 2004;39:432–439. [PubMed: 14743149]
12. Misra S, Lee N, Fu A, et al. Increased expression of a disintegrin and metalloproteinase thrombospondin-1 (ADAMTS-1) in thrombosed hemodialysis grafts. J Vasc Interv Radiol 2008;19:111–119. [PubMed: 18192475]
13. Luque A, Carpizo DR, Iruela-Arispe ML. ADAMTS1/METH1 inhibits endothelial cell proliferation by direct binding and sequestration of VEGF165. J Biol Chem 2003;278:23656–23665. [PubMed: 12716911]
14. Rotmans JI, Pattynama PMT, Verhagen HJM, et al. Sirolimus-eluting stents to abolish intimal hyperplasia and improve flow in porcine arteriovenous grafts: A 4-Week follow-up study. Circulation 2005;111:1537–1542. [PubMed: 15781738]
15. Rotmans JI, Verhagen HJ, Velema E, et al. Local overexpression of C-type natriuretic peptide ameliorates vascular adaptation of porcine hemodialysis grafts. Kidney Int 2004;65:1897–1905. [PubMed: 15086933]
16. Weiss MF, Scivittaro V, Anderson JM. Oxidative stress and increased expression of growth factors in lesions of failed hemodialysis access. Am J Kidney Dis 2001;37:970–980. [PubMed: 11325679]
17. Castier Y, Lehoux S, Hu Y, Fonteinos G, Tedgui A, Xu Q. Characterization of neointima lesions associated with arteriovenous fistulas in a mouse model. Kidney Int 2006;70:315–320. [PubMed: 16760906]
18. Yang B, Shergill U, Fu AA, Knudsen B, Misra S. The mouse arteriovenous fistula model. J Vasc Interv Radiol 2009;20:946–950. [PubMed: 19555889]
19. Committee on care and use of laboratory animals of the institute of laboratory animal resources. Washington, DC: Government print office; 1996.
20. Misra S, Fu A, Rajan D, et al. Expression of hypoxia inducible factor-1 alpha, macrophage migration inhibition factor, matrix metalloproteinase-2 and -9, and their inhibitors in hemodialysis grafts and arteriovenous fistulas. J Vasc Interv Radiol 2008;19:252–259. [PubMed: 18341958]

21. Misra S, Fu A, Anderson J, Glockner J, et al. The rat femoral arteriovenous fistula model: Increased expression of MMP-2 and MMP-9 at the venous stenosis. J Vasc Interv Radiol 2008;19:587–594. [PubMed: 18375305]
22. Pawlak K, Pawlak D, Mysliwiec M. Circulating beta-chemokines and matrix metalloproteinase-9/tissue inhibitor of metalloproteinase-1 system in hemodialyzed patients--role of oxidative stress. Cytokine 2005;31:18–24. [PubMed: 15896974]
23. Pawlak K, Pawlak D, Mysliwiec M. Possible association between circulating vascular endothelial growth factor and oxidative stress markers in hemodialysis patients. Med Sci Monit 2006;12:CR181–CR185. [PubMed: 16572054]
24. Kren S, Hostetter TH. The course of the remnant kidney model in mice. Kidney Int 1999;56:333–337. [PubMed: 10411710]
25. Misra S, Gordon JD, Fu AA, et al. The porcine remnant kidney model of chronic renal insufficiency. J Surg Res 2006;135:370–379. [PubMed: 16815448]
26. Misra S, Fu AA, Anderson JL, et al. Fetuin-A expression in early venous stenosis formation in a porcine model of hemodialysis graft failure. J Vasc Interv Radiol 2008;19:1477–1482. [PubMed: 18693047]
27. Hueper WC. Atherosclerosis: the anoxemia theory. Arch Pathol 1944;28:173–205.
28. Moreno PR, Purushothaman K-R, Sirol M, Levy AP, Fuster V. Neovascularization in human atherosclerosis. Circulation 2006;113:2245–5222. [PubMed: 16684874]
29. Jonsson-Rylander A-C, Nilsson T, Fritsche-Danielson R, et al. Role of ADAMTS-1 in atherosclerosis: remodeling of carotid artery, immunohistochemistry, and proteolysis of versican. Arterioscler Thromb Vasc Biol 2005:180–185. [PubMed: 15539621]
30. Bongrazio M, Baumann C, Zakrzewicz A, Pries AR, Gaehtgens P. Evidence for modulation of genes involved in vascular adaptation by prolonged exposure of endothelial cells to shear stress. Cardiovasc Res 2000;47:384–393. [PubMed: 10946075]
31. Misra S, Woodrum D, Homburger J, et al. Assessment of wall shear stress changes in arteries and veins of arteriovenous polytetrafluoroethylene grafts using magnetic resonance imaging. Cardiovasc Intervent Radiol 2006;29:624–629. [PubMed: 16729233]
32. Misra S, Fu A, Misra K, Glockner J, Mukhopadhyay D. Wall shear stress measurement using phase contrast magnetic resonance imaging with phase contrast magnetic resonance angiography in arteriovenous polytetrafluoroethylene grafts. Angiology 2009;60:441–447. [PubMed: 19625275]

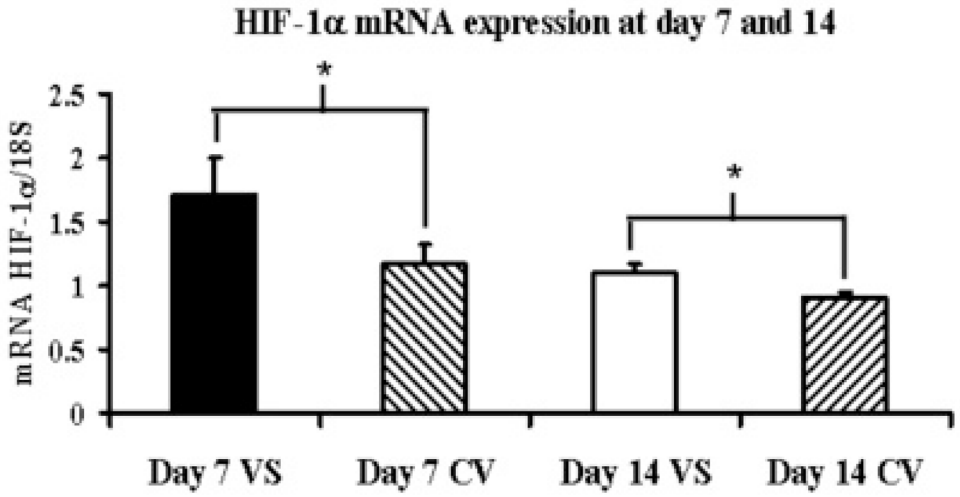

Fig. 1.

Gene expression of HIF-1α at the venous stenosis and control vessel at day 7 and 14 after fistula creation. Pooled data for the four mice at day 7 and 14. Data are mean ± SD. (*) is $P<0.05$.

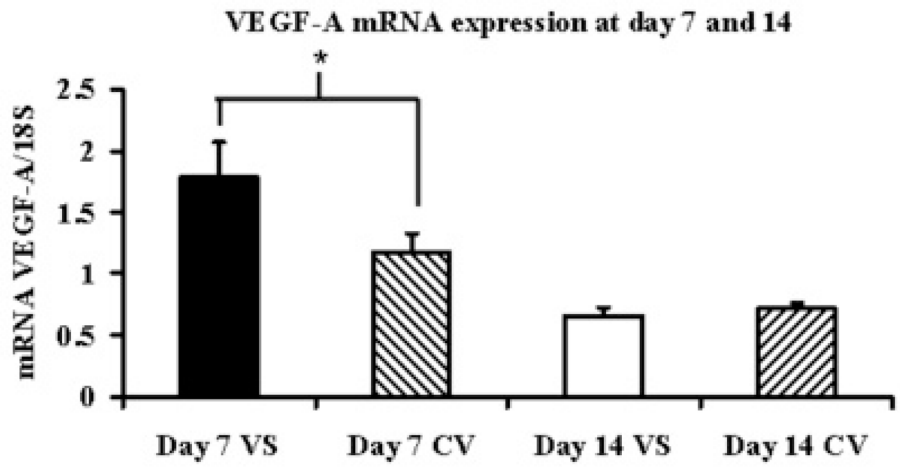

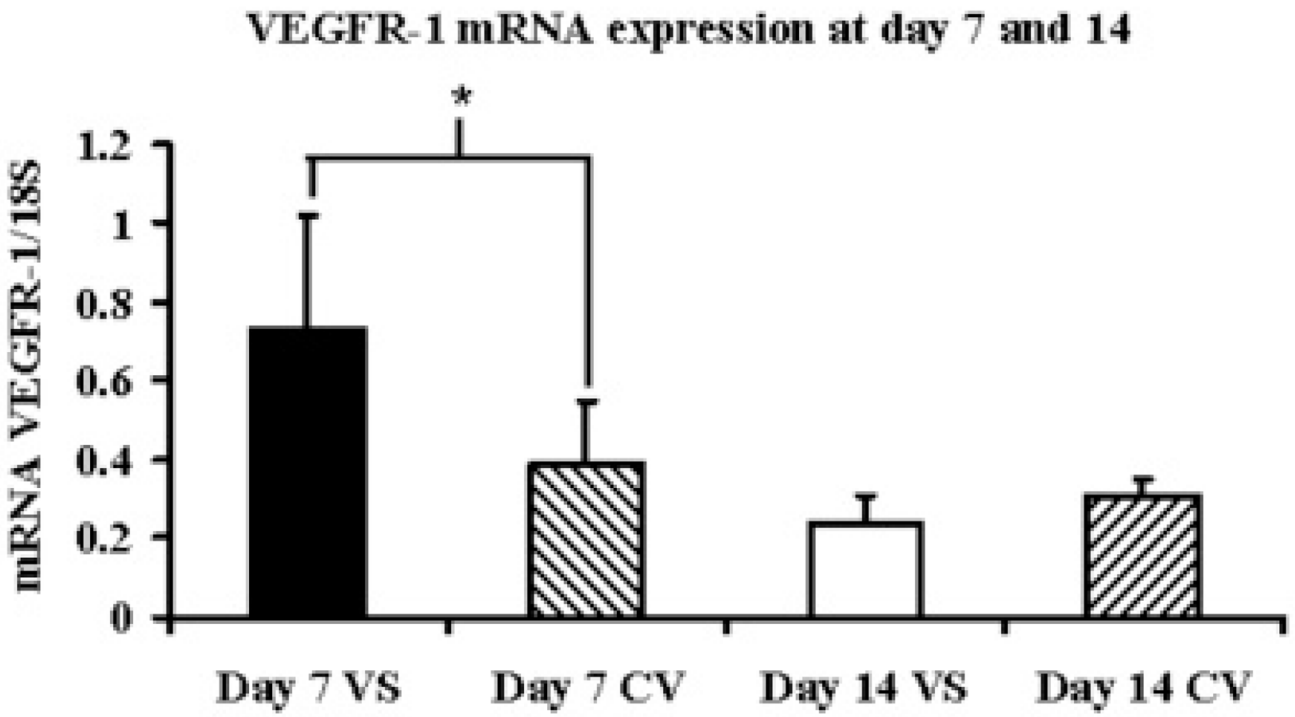

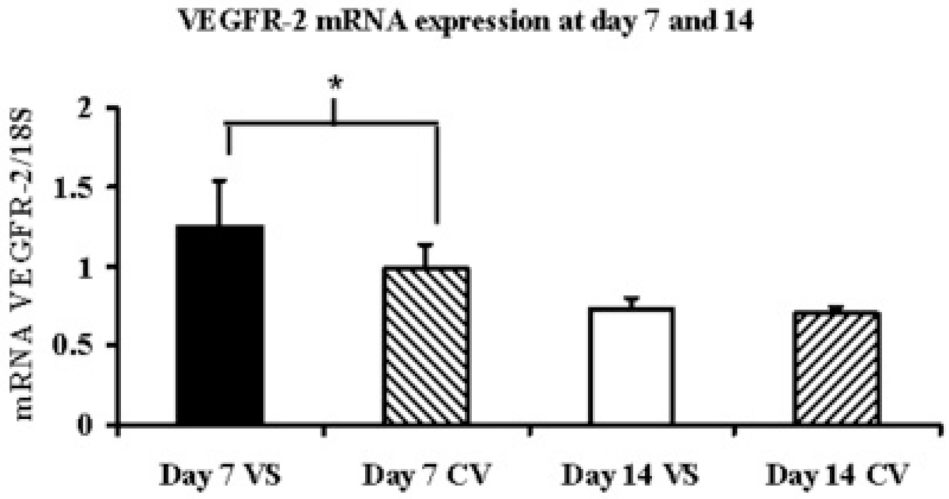

Fig. 2.

Gene expression of VEGF-A **(A)**, VEGFR-1 **(B)**, and VEGFR-2 **(C)** at the venous stenosis (VS) and control vein (CV) at day 7 and 14after fistula creation. Pooled data for the four mice at day 7 and 14. Data are mean ± SD. (*) is $P<0.05$.

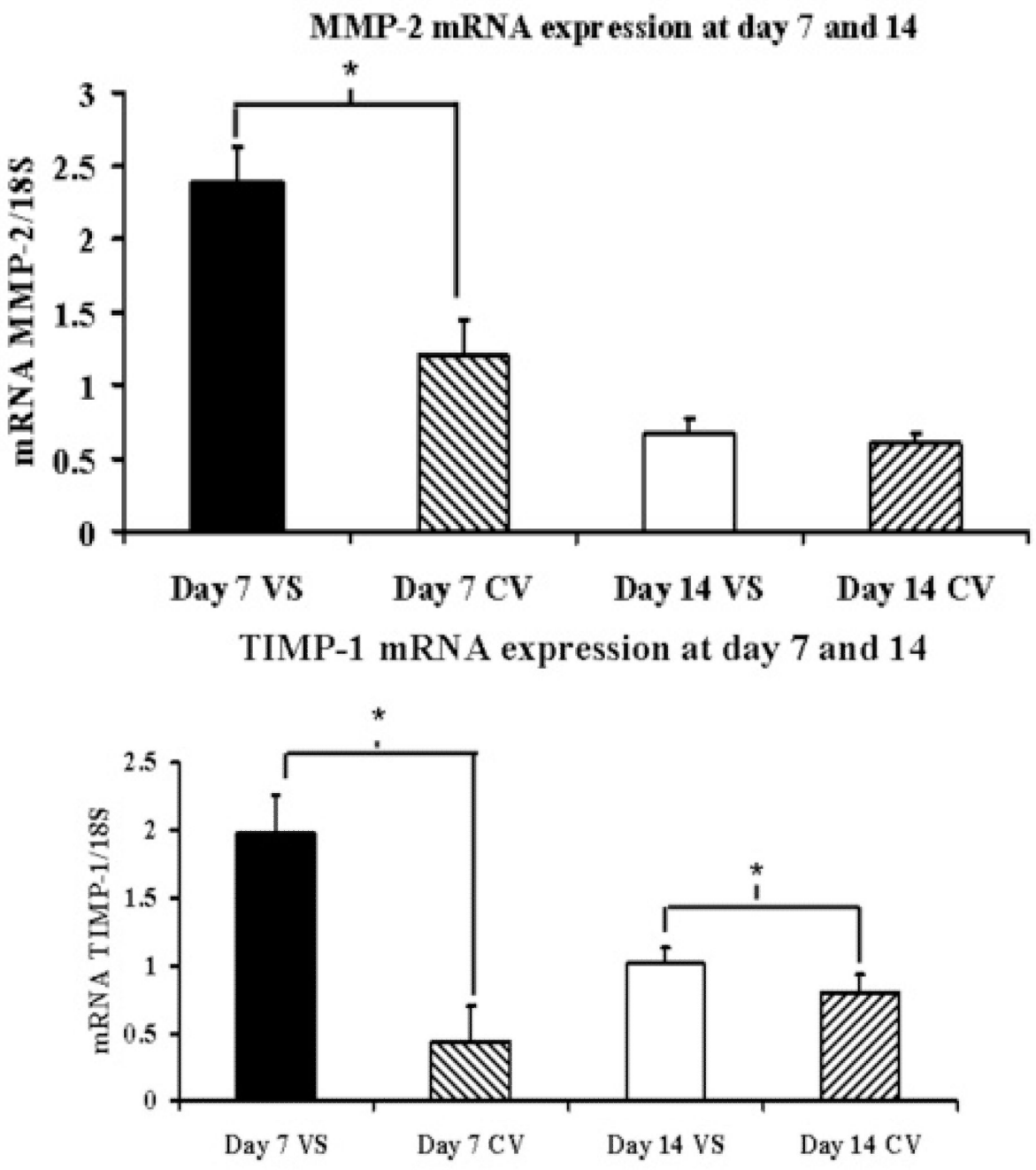

Fig. 3.

Gene expression of MMP-2 **(A)** and TIMP-1 **(B)** at the venous stenosis (VS) and control vein (CV) at day 7 and 14 after fistula creation. Pooled data for the four mice at day 7 and 14. Data are mean ± SD. (*) is $P<0.05$.

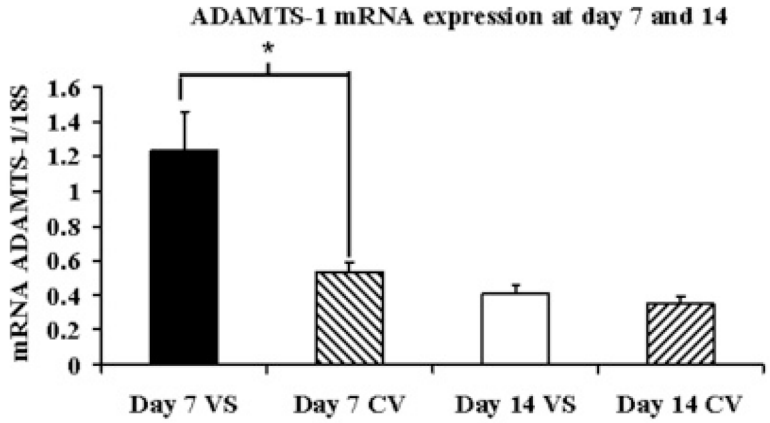

Fig. 4.

Gene expression of ADAMTS-1 at the venous stenosis (VS) and control vein (CV) at day 7 and 14 after fistula creation. Pooled data for the four mice at day 7 and 14. Data are mean ± SD. (*) is $P<0.05$.

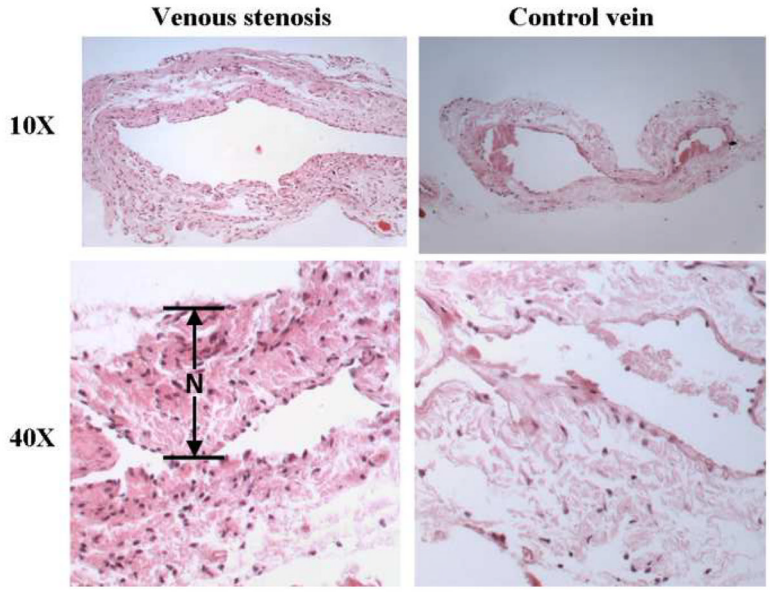

Fig. 5.
Hematoxylin and eosin (H and E) staining of the venous stenosis and control vein at day 28 showing a thickened neointima (N) with hypercellularity when compared to the control vein.

Table 1

Gene	Sequence	Amplicon Length	Cycles
MMP-2	5′ – agatcttcttcttcaaggaccggtt– 3′ (sense) 5′ – ggctggtcagtggcttggggta– 3′ (antisense)	225	35
MMP-9	5′ – gtttttgatgctattgctgagatcca– 3′ (sense) 5′ – cccacatttgacgtccagagaagaa3′ (antisense)	208	35
TIMP-1	5′ – ggcatcctcttgttgctatcactg– 3′ (sense) 5′ – gtcatcttgatctcatcccgctgg– 3′ (antisense)	169	35
TIMP-2	5′ – ctcgctggacgttggaggaaagaa– 3′ (sense) 5′ – agcccatctggtacctgtggttca– 3′ (antisense)	155	35
HIF-1α	5′ –agtgatgaaagaattact– 3′ (sense) 5′ –aataataccacttacaaca– 3′ (antisense)	2759	35
VEGF-A	5′ –atgaagtgatcaagttcatgg– 3′ (sense) 5′ –ggatcttggacaaacaaatgc– 3′ (antisense)	360	35
VEGFR-1	5′ –tttccatttgatactcttac– 3′ (sense) 5′ –tcttagttgctttaccaggg– 3′ (antisense)	310	35
VEGFR-2	5′ –tgtggttgtaggatataggat– 3′ (sense) 5′ –aaaggctttgtgtgaactcgg– 3′ (antisense)	338	35
ADAMTS-1	5′ –cattaacggacaccctgctt– 3′ (sense) 5′ –cgtgggacacacatttcaag– 3′ (antisense)	166	35
18S	5′ –agctaggaataatggaatag– 3′ (sense) 5′-aatcaagaacgaaagtcggag- 3′ (antisense)	150	19